UNIVERSITY OF AMSTERDAM

UvA-DARE (Digital Academic Repository)

Growth kinetic parameters of two planktonic desmid species under fluctuating phosphorus conditions in continuous-flow culture.

Spijkerman, E.; Coesel, P.F.M.

DOI
10.1093/plankt/19.12.1899

Publication date
1997

Published in
Journal of plankton research

Link to publication

Citation for published version (APA):
Spijkerman, E., & Coesel, P. F. M. (1997). Growth kinetic parameters of two planktonic desmid species under fluctuating phosphorus conditions in continuous-flow culture. *Journal of plankton research*, *19*, 1899-1912. https://doi.org/10.1093/plankt/19.12.1899

General rights
It is not permitted to download or to forward/distribute the text or part of it without the consent of the author(s) and/or copyright holder(s), other than for strictly personal, individual use, unless the work is under an open content license (like Creative Commons).

Disclaimer/Complaints regulations
If you believe that digital publication of certain material infringes any of your rights or (privacy) interests, please let the Library know, stating your reasons. In case of a legitimate complaint, the Library will make the material inaccessible and/or remove it from the website. Please Ask the Library: https://uba.uva.nl/en/contact, or a letter to: Library of the University of Amsterdam, Secretariat, P.O. Box 19185, 1000 GD Amsterdam, The Netherlands. You will be contacted as soon as possible.

UvA-DARE is a service provided by the library of the University of Amsterdam (https://dare.uva.nl)

Download date:15 Oct 2026

Journal of Plankton Research Vol.19 no.12 pp.1899–1912, 1997

Growth kinetic parameters of two planktonic desmid species under fluctuating phosphorus conditions in continuous-flow culture

Elly Spijkerman and Peter F.M.Coesel

Department of Aquatic Ecology, University of Amsterdam, Kruislaan 320, NL-1098 SM Amsterdam, The Netherlands

Abstract. Two planktonic desmid taxa, *Staurastrum chaetoceras* and *Cosmarium abbreviatum* var. *planctonicum*, were examined under pulsed phosphorus (P)-limited conditions in continuous culture. Two pulse regimes were applied, i.e. 2.5 µM P twice a week and 10 µM P once every 2 weeks. Under both pulse regimes, *S.chaetoceras* showed a higher maximum P uptake rate (V_{max}) and affinity for P uptake (V_{max}/affinity constant K_m) than *C.abbreviatum*. Affinity for P uptake in *S.chaetoceras* just before pulsing was higher than shortly after pulsing, whereas *C.abbreviatum* did not show any significant difference. Cell densities and cellular P quota in *S.chaetoceras* and *C.abbreviatum* fluctuated in a comparable way, but fluctuations in *C.abbreviatum* were less pronounced than in *S.chaetoceras*. The mean cell volume of both species was greater under the bimonthly than under the biweekly pulse regime, and the lowest under continuous P-limited conditions. Competition between *S.chaetoceras* and *C.abbreviatum* under the bimonthly pulse regime was won by *S.chaetoceras*, but displacement was less fast than under more frequent pulsing (equalling the same total P supply). The above-mentioned results are discussed in relation to possible ecological strategies.

Introduction

Algal cells living in an unstable environment are continuously subjected to a fluctuating nutrient supply. Periods of superfluous availability of a growth-limiting nutrient may be interspersed with periods of shortage (e.g. Sommer, 1991a,b). Although we are convinced of the causal relationship between fluctuating nutrient concentrations and algal population dynamics in the field, this is hardly reflected in relevant experimental research. When predicting the growth of one or more species during fluctuating nutrient supply, often physiological data from growth in steady-state continuous nutrient-limited conditions are used (Grover, 1988, 1991; Olsen *et al.*, 1989), ignoring any physiological changes resulting from the pulsed supply regime.

In order to study possible adaptation in phosphorus (P) uptake kinetics and growth response, we cultured two desmid species under two different, fluctuating P regimes. The two desmid species, *Staurastrum chaetoceras* and *Cosmarium abbreviatum*, originated from trophically different alkaline lakes and have been well characterized in their growth kinetic parameters under continuous P limitation (Spijkerman and Coesel, 1996b).

Under continuous P limitation, we found *S.chaetoceras* to have a higher maximum initial uptake rate (V_{max}) and *C.abbreviatum* to have a higher affinity for uptake, i.e. V_{max}/affinity constant K_m (Spijkerman and Coesel, 1996b). Because the internal P quotas were comparable between the two species under these conditions, the difference found in uptake kinetics led to a higher affinity for growth of *C.abbreviatum* under stringent P limitation ($\mu < 0.012$ h^{-1}), compared to *S.chaetoceras*. Under less stringent P limitation ($\mu > 0.012$ h^{-1}),

© Oxford University Press

S.chaetoceras had the higher affinity for growth and these results were in agreement with the outcome of competition between these two species under different conditions of continuous P limitation (Spijkerman and Coesel, 1996b). Besides this, we found maximum uptake rates measured over a longer time period (20 min) in cells grown under continuous P limitation to be higher in *C.abbreviatum* than in *S.chaetoceras* (E.Spijkerman and P.F.M.Coesel, submitted). This characteristic is of importance when algal cells are subjected to a saturating pulse. The present paper deals with intermediate conditions between continuous P limitation and a saturating pulse.

Method

The experiments were performed with *S.chaetoceras* (Sch.) G.M. Smith, clone AO 36, isolated from the alkaline eutrophic Lake IJsselmeer (Berger and Sweers, 1988) and *C.abbreviatum* Rac. var. *planctonicum* W. & G. S. West, clone AO 116, isolated from the alkaline, oligomesotrophic Lake Maarsseveen (I) (Swain *et al.*, 1987), both lakes being located in the Netherlands. Clones were taken from the desmid collection at our department.

Culture conditions and analytical methods

The species were cultured at 20 ± 1°C in 1 l continuous-flow culture vessels. For details about the continuous-flow device, see Coesel and Wardenaar (1994). Circular fluorescent tubes provided an average photosynthetically active radiation (PAR) in the culture vessel of 140–200 μmol m^{-2} s^{-1}, which proved to be saturating for growth. Illumination of the unialgal cultures was continuous. The inflow medium contained no P, but did contain 36 μM Fe (added as Fe–EDTA complex). Other nutrients were added as described in Spijkerman and Coesel (1996a). The N:P ratio (by atoms) was always >800 or >200 during the 2.5 or 10 μM P pulse regime, respectively. The dilution rate (D) was set at 0.007 h^{-1} for every culture condition described and P was added directly in the culture vessel from a sterilized stock solution. Two pulse regimes were applied: 2.5 μM P twice a week and 10 μM P once every 2 weeks, resulting in a total weekly P supply comparable to that in continuously P-limited cultures at the same dilution rate (5 μmol P l^{-1}). Cultures were not axenic, but bacterial biomass (estimated by acridine staining and counting under a fluorescence microscope) was negligible (<1% of algal biomass). Algal cells were counted and cell volumes estimated with a Coulter Multisizer. From every culture condition, cell volumes of at least 50 individuals of each species were measured microscopically by use of appropriate geometric formulae. As to *C.abbreviatum*, the cell suspension was coloured with Indian ink, highlighting the extracellular mucus layer; the thickness of this layer (at the apex) was measured separately. Growth rates were calculated over different time intervals during the pulse regime. In the 2.5 μM P pulse regime two intervals (day 0–2 and 2–3.5), and in the 10 μM P pulse experiment five intervals (day 0–2, 2–4, 4–7, 7–9 and 9–14), were distinguished in which growth was calculated. After the addition of a pulse, a time delay was often observed before growth resumed.

These delays were estimated by fitting an exponential curve on the decrease as well as one on the increase in cell density. The period from the pulse to the intercept was taken as the time delay.

Protein was measured according to Lowry *et al.* (1951). Cellular P concentrations were determined in the pellet after centrifugation (1500 *g*, 10 min); total cellular P was measured after digestion with $K_2S_2O_8$ (added in excess) and 0.15 M H_2SO_4 in sealed glass tubes at 100°C for 1 h. The external soluble reactive phosphorus (SRP) was assessed from the supernatant after centrifugation (1500 *g*, 10 min). Both fractions were measured according to Murphy and Riley (1962). By dividing total cellular P concentration by cell density, cellular P quotas (Q_p) were obtained. Tests for significance were carried out following Sokal and Rohlf (1981).

Uptake experiments

Uptake experiments were performed with single-species culture material, just before and 24 h after the addition of a pulse. In the case of the 2.5 μM P pulse, uptake experiments were also performed 1 h after the pulse because the pulse was just consumed at this time, comparable to 24 h after the 10 μM P pulse. Culture material was diluted 2-fold with P-free culture medium and pulsed with different inorganic phosphorus (P_i) concentrations containing ^{32}P as described in Spijkerman and Coesel (1996a). Initial P_i concentrations ranged from 0.5 to 30 μM. Cellular ^{32}P contents were determined at t = 0, 30, 60 and 300 s, and initial uptake rates (V) for every initial P_i concentration were calculated from a linear regression, following Riegman and Mur (1984). By curve fitting to the Michaelis–Menten equation

$$V = V_{max}(P_i/(K_m + P_i)) \quad (1)$$

the maximum uptake rate (V_{max}) and half-saturation constant for uptake (K_m) were computed.

Competition experiment

A discontinuously P-limited competition experiment with *C.abbreviatum* and *S.chaetoceras* was carried out at D = 0.007 h^{-1}. P (10 μM) was added once every 2 weeks, comparable to the single-species culture. To resemble natural conditions more closely, illumination in the competition experiment was applied under a 16:8 h light:dark regime. Pulses were always supplied during the light period. Other growth conditions were as described for single-species chemostat cultures. Algal strains were pre-cultured in chemostats under the target P limitation. Experiments were then started by mixing the two species in a 1:1 cell number ratio. Cell numbers were counted three times a week using a 1 ml capacity Sedgewick–Rafter cell. The rate at which one species was replaced by the other was estimated by fitting an exponential curve on the relative decrease of one of the species over time. This replacement rate was compared with those derived

from previous competition experiments carried out under other conditions of P limitation (Spijkerman and Coesel, 1996b).

Results

P uptake kinetics in single-species cultures

Both with the 2.5 and 10 μM P pulse regime, maximum initial uptake rates (V_{max}) and affinities (V_{max}/K_m) were significantly higher in *S.chaetoceras* than in *C.abbreviatum* (Table I, ANOVA, $P < 0.001$). In *C.abbreviatum*, the affinity constant (K_m) before and after each pulse was about the same (ANOVA, $P = 0.965$), but in *S.chaetoceras* after each pulse, when the external P_i concentration was just exhausted, K_m was higher compared to before (Mann–Whitney U, $P < 0.05$). This resulted in a lower affinity for *S.chaetoceras* after the pulse than before. When P was exhausted for a longer period (24 h after the 2.5 μM P pulse), the affinity constant was comparable to the initial values again (ANOVA, $P = 0.759$).

Course of Q_p in single-species cultures

To standardize the data, Q_p at the time of the pulse was set to 100% for both species (Figure 1A and B). After a pulse was given, the external P was taken up very quickly by *S.chaetoceras* and *C.abbreviatum*, partly filling their internal stores. In the 2.5 μM P pulse regime, *S.chaetoceras* could reach a higher Q_p than *C.abbreviatum* (Figure 1A) because the culture contained a somewhat lower cell density compared to the culture of *C.abbreviatum* (Figure 2A). When the data were corrected for this difference in pulse size per cell, no differences in Q_p between *S.chaetoceras* and *C.abbreviatum* could be observed. In the 10 μM P pulse experiment, *C.abbreviatum* attained its maximum Q_p later than *S.chaetoceras* (Figure 1B).

Course of cell density in single-species cultures

Considering the fluctuating cell density in the pulsed cultures, differences between *C.abbreviatum* and *S.chaetoceras* can be observed (Figures 2 and 3). In

Table I. Maximum initial uptake rates (V_{max}, μmol P mg^{-1} protein h^{-1}), affinity constants (K_m, μmol P l^{-1}) and affinities (V_{max}/K_m) for *C.abbreviatum* and *S.chaetoceras* before and after pulses of 2.5 and 10 μM P. Means ± SD, n = number of replicates

	C.abbreviatum				*S.chaetoceras*			
	V_{max}	K_m	V_{max}/K_m	n	V_{max}	K_m	V_{max}/K_m	n
2.5 μM P pulse								
Before	0.68 ± 0.21	6.61 ± 1.99	0.10 ± 0.00	2	0.97 ± 0.20	3.10 ± 0.29	0.32 ± 0.09	2
After 1 h	0.66 ± 0.38	7.74 ± 1.63	0.08 ± 0.03	2	1.32	7.64	0.17	1
After 24 h	0.59 ± 0.10	6.31 ± 0.15	0.09 ± 0.01	2	1.02 ± 0.01	3.19 ± 0.77	0.33 ± 0.08	2
10 μM P pulse								
Before	0.59 ± 0.19	6.29 ± 3.63	0.10 ± 0.03	3	1.39 ± 0.38	3.57 ± 0.42	0.40 ± 0.15	2
After 24 h	0.46 ± 0.31	5.03 ± 1.53	0.09 ± 0.04	2	0.99 ± 0.20	6.06 ± 2.55	0.17 ± 0.04	2

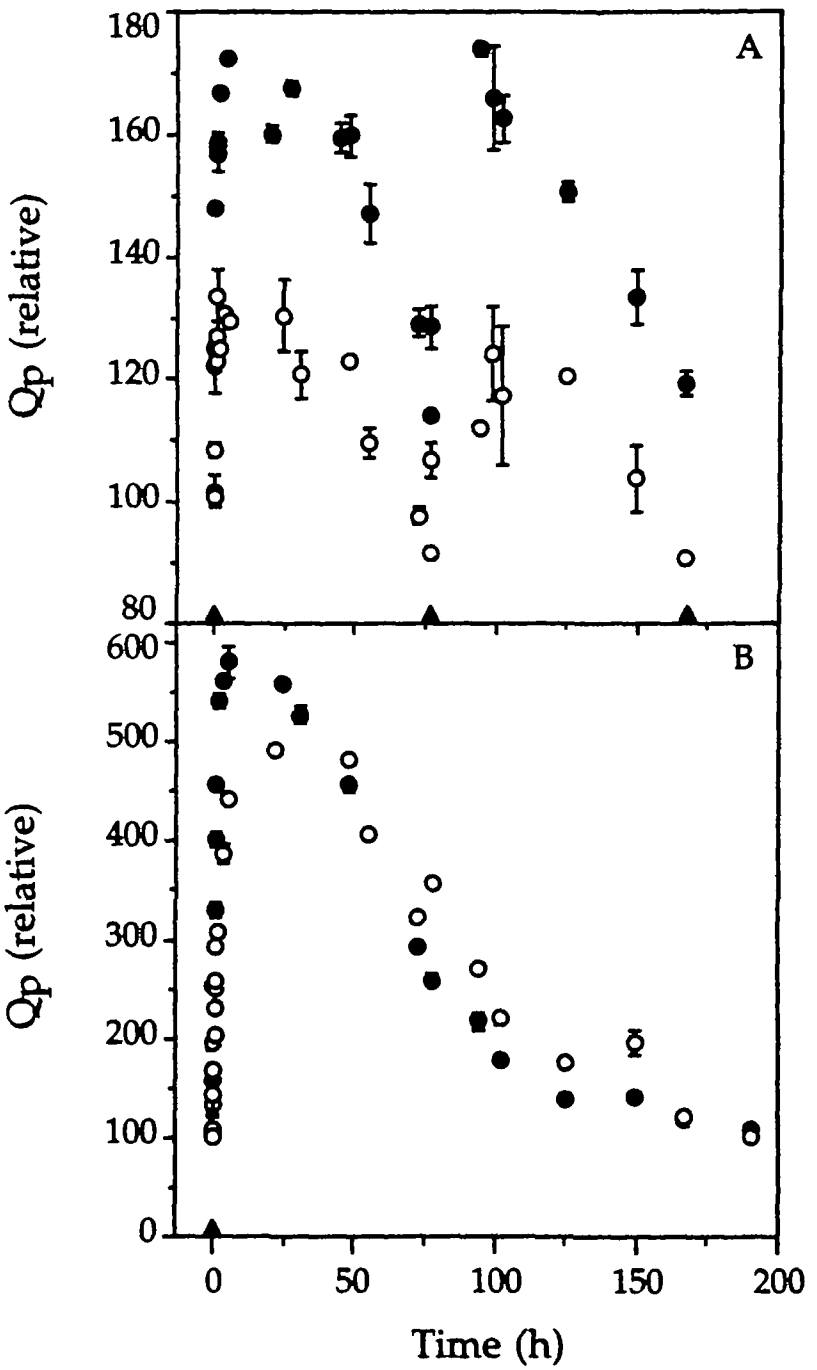


Fig. 1. Evolution of cellular P quota (Q_p) relative to Q_p at time 0 (= 100%) of *C.abbreviatum* (○) and *S.chaetoceras* (●) in the pulsed P-limited monocultures. Phosphorus pulses are indicated by triangles on the abscissa: (**A**) 2.5 μM P pulse; (**B**) 10 μM P pulse.

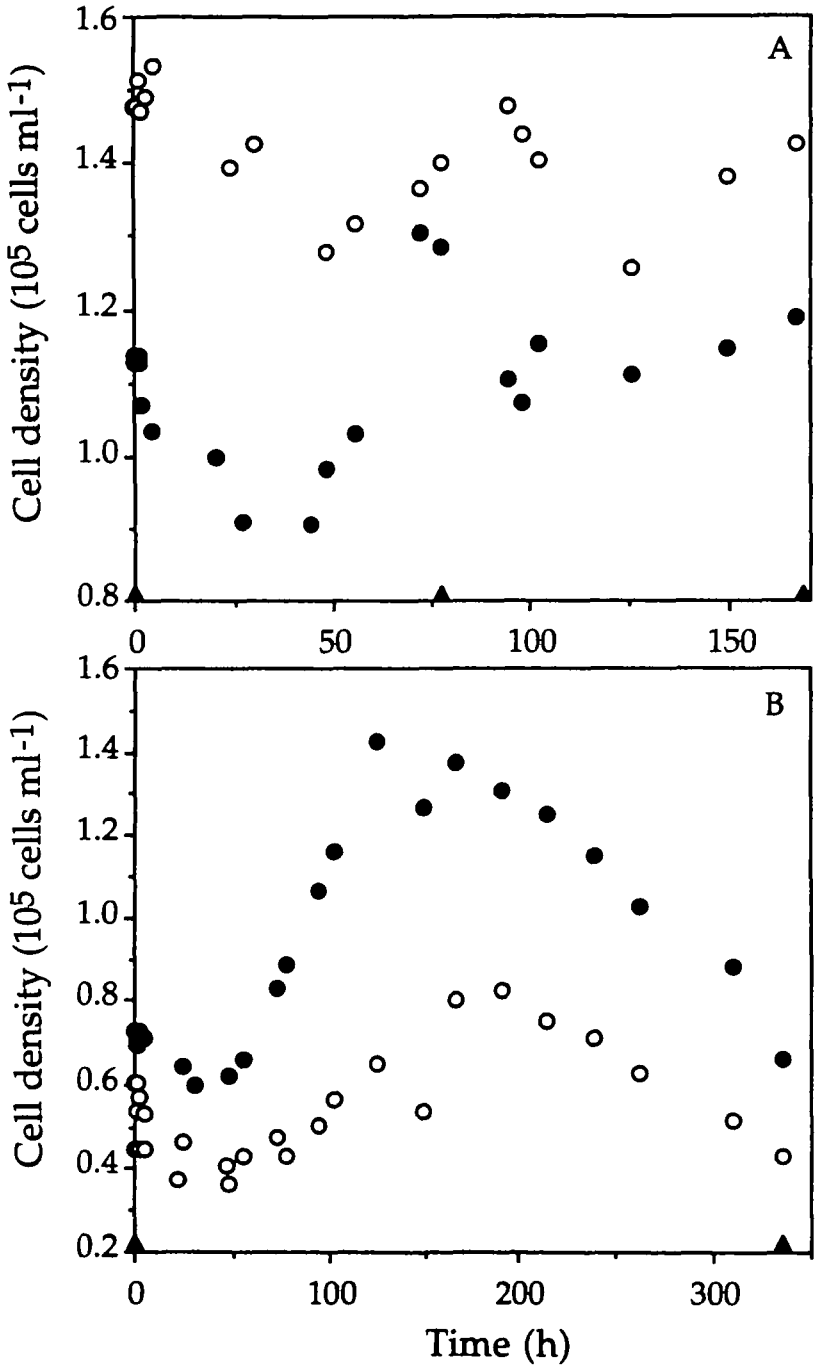


Fig. 2. The course of cell density of *C.abbreviatum* (○) and *S.chaetoceras* (●) during the monoculture experiments. Phosphorus pulses are indicated by triangles on the abscissa: (**A**) 2.5 µM P pulse; (**B**) 10 µM P pulse.

Table II. Growth rates on the basis of cell numbers (μ, h^{-1}) of *C.abbreviatum* and *S.chaetoceras* over different time intervals (d = day number) in the single-species continuous-flow cultures ($D = 0.007\ h^{-1}$). Two pulse regimes were used: addition of 2.5 µM P twice a week and 10 µM P once every 2 weeks. The average ± SD and number of replicates (n) are given

	C.abbreviatum μ (h^{-1})	*S.chaetoceras* μ (h^{-1})
2.5 µM P		
d 0–2	0.006 ± 0.003 (25)	0.004 ± 0.002 (26)
d 2–3.5	0.008 ± 0.002 (32)	0.009 ± 0.003 (36)
10 µM P		
d 0–2	0.005 ± 0.003 (14)	0.004 ± 0.004 (10)
d 2–4	0.014 ± 0.003 (14)	0.017 ± 0.004 (11)
d 4–7	0.011 ± 0.002 (15)	0.012 ± 0.004 (11)
d 7–9	0.006 ± 0.002 (14)	0.005 ± 0.002 (10)
d 9–14	0.004 ± 0.002 (28)	0.002 ± 0.004 (20)

the 2.5 µM P pulse experiment, fluctuations in the cell density of both species seemed to be independent of the pulse regime (Figure 3A). When calculating growth rates on the basis of cell numbers for the different time intervals (Table II), it is shown that in the period following the pulse (day 0–2) *C.abbreviatum* achieved a significantly higher growth rate than *S.chaetoceras* (ANOVA, $P < 0.001$), whereas *S.chaetoceras* had a higher growth rate in the period of day 2–3.5 (ANOVA, $P < 0.05$). With the 10 µM P pulse regime, both species often showed a decrease in growth rate right after the pulse (Figure 3B; Table II). Another observed phenomenon is the less pronounced fluctuation in cell density in *C.abbreviatum* compared to *S.chaetoceras* in the 10 µM P pulse experiment (Figure 3B). Particularly in the period of day 2–4, *S.chaetoceras* displayed a distinctly higher growth rate than *C.abbreviatum* (Table II, ANOVA, $P < 0.05$).

Cell volumes in single-species cultures

Although in both species mean cell volumes fluctuated somewhat during the pulse regime, no significant differences were found between any of the days following the pulse (not shown). However, for both *S.chaetoceras* and *C.abbreviatum*, an increase in cell volume measured by the Coulter counter was observed, starting from continuously P-limited conditions with increasing pulse dose (Table III, Kruskal–Wallis, $P < 0.001$). This was confirmed by measurements under the microscope. Microscopic measurements of cell volumes of *S.chaetoceras* were found to be about equal to those of the Coulter counter (95–115%), whereas cell volumes of *C.abbreviatum* measured under the microscope were only 70–75% of those given by the Coulter device. As it can reasonably be expected that the size of *S.chaetoceras* is more readily miscalculated by either method because of the more complicated shape of the cells (six arms on two conical semi-cell bodies) compared to those of *C.abbreviatum* (two ellipsoid semi-cells), we conclude that the Coulter counter presumably overestimates the average cell volume of *C.abbreviatum* because it is influenced by its mucus layer. This mucus layer in *C.abbreviatum* was found to increase with pulse dose as well (Table III).

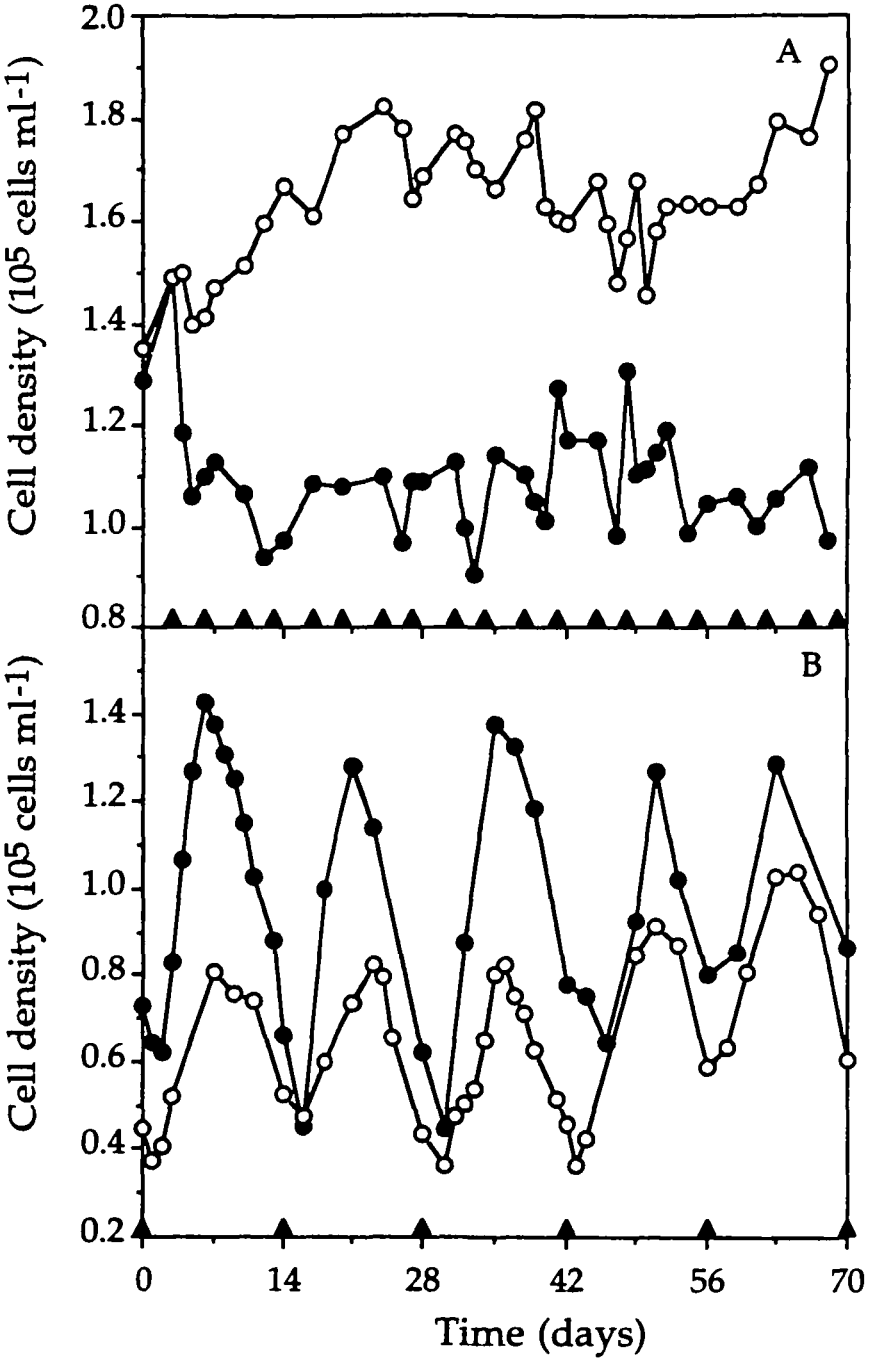


Fig. 3. Population dynamics of *C.abbreviatum* (○) and *S.chaetoceras* (●) during the monoculture experiments with repeating pulses. Phosphorus pulses are indicated by triangles on the abscissa: (**A**) 2.5 μM P pulse; (**B**) 10 μM P pulse.

Table III. Average cell volume (μm^3 ± SD) of *C.abbreviatum* and *S.chaetoceras*, as well as the thickness of the mucus layer in *C.abbreviatum* (µm ± SD) at different culture conditions. Both Coulter and microscopic measurements are given. The number of Coulter-counted replicates is given in parentheses

	C.abbreviatum			*S.chaetoceras*			*C.abbreviatum*
	Cell volume			Cell volume			Mucus layer
	Microscope	Coulter		Microscope	Coulter		Microscope
Continuous P limitation (μ = 0.003–0.007 h^{-1})	2504 ± 439	3386 ± 695	(12)	1828 ± 492	1725 ± 111	(5)	22 ± 4
2.5 µM P pulse	3300 ± 501	4237 ± 163	(106)	1903 ± 328	2149 ± 127	(100)	29 ± 2
10 µM P pulse	3215 ± 537	4672 ± 250	(92)	2234 ± 519	2572 ± 151	(75)	28 ± 3

Competition experiment and replacement rates

Competition for a large pulse (10 µM P) between *S.chaetoceras* and *C.abbreviatum* resulted in a dominance for *S.chaetoceras*, gradually replacing *C.abbreviatum* during the experiment (Figure 4). Like in the single-species experiments, the

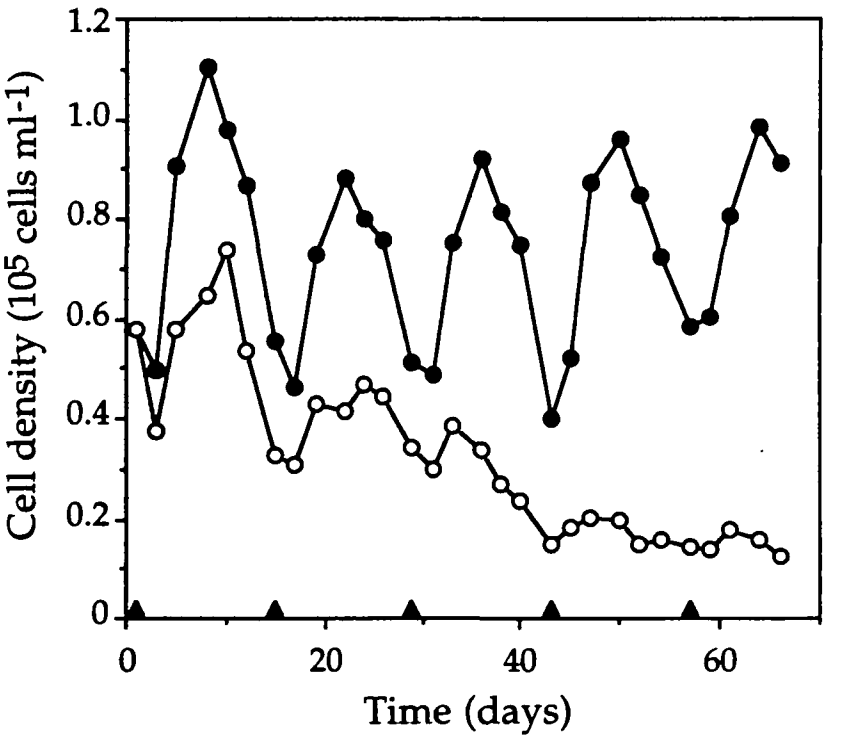


Fig. 4. Population dynamics of *C.abbreviatum* (○) and *S.chaetoceras* (●) during the competition experiments. Phosphorus pulses are indicated by triangles on the abscissa.

fluctuations in cell density were greater in *S.chaetoceras* than *C.abbreviatum*. When considering the range from continuous P limitation towards a pulsed P limitation with increasing pulse size (and increasing time interval, resulting in a constant total weekly P supply), an optimum for *S.chaetoceras* can be noticed at intermediate pulse size versus an optimum for *C.abbreviatum* at continuous P limitation (Figure 5).

Discussion

Regarding the competitive position of phytoplankton species under pulsed P conditions, the following characteristics in particular may be considered relevant: maximum uptake rate, storage capacity, possible lag period in growth and maximum growth rate on stored P.

For both *C.abbreviatum* and *S.chaetoceras*, we observed an adaptation in V_{max} and K_m comparing uptake kinetics under pulsed P limitation with continuous P limitation (Spijkerman and Coesel, 1996b). In both species, V_{max} increased in the pulsed P-limited cultures, thus enabling a better utilization of the pulse. The affinity for uptake decreased drastically in *C.abbreviatum* and increased in

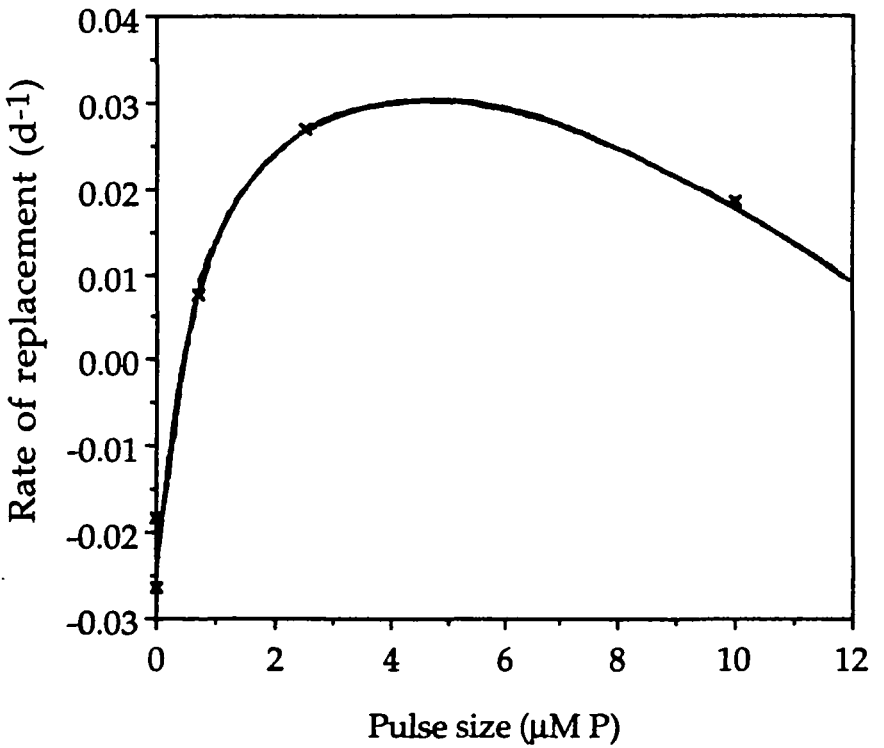


Fig. 5. Rate of replacement (day^{-1}) of *C.abbreviatum* by *S.chaetoceras* under different P-limited conditions with equal total weekly P supply.

S.chaetoceras. This indicates that compared to the uptake kinetics found under continuous P limitation (Spijkerman and Coesel, 1996b), *C.abbreviatum* does not invest cellular energy in high affinity for uptake, but in maximum uptake rate of large pulses. The higher affinity in *S.chaetoceras*, however, indicates an adaptation towards the uptake of relatively small pulses. V_{max} (and K_m) in *C.abbreviatum* before and after the pulse were about the same. A different response was found in *S.chaetoceras*, where V_{max} remained constant, but K_m was found to be higher when the pulse had just been consumed. This result indicates a fast adaptive ability of *S.chaetoceras* to a changing environment. Grover (1991) found V_{max} to be independent of Q_p, but measured only 2 days after the pulse. This could have influenced his results because we noticed that a change in P_i uptake characteristics was confined to the period of actual uptake. Quarmby *et al.* (1982) found that *Skeletonema costatum* and *Chaetoceros gracile* growing under pulsed additions of ammonium had both a higher initial uptake rate ($V_{i,max}$) and a higher maximum long-term uptake rate ($V_{lt,max}$) than when ammonium was supplied continuously. They stated that an adaptation in $V_{i,max}$ would be of advantage in environments where a high frequency of small pulses is common and that an increase in $V_{lt,max}$ would be advantageous in habitats where nutrient patches are of long duration. We found that under continuously P-limited conditions, the $V_{lt,max}$ in *C.abbreviatum* was distinctly higher than that in *S.chaetoceras*, thus favouring its occurrence under conditions of infrequent, large pulses (E.Spijkerman and P.F.M.Coesel, submitted).

When pulses of P were given to cells originating from continuously P-limited cultures, a time lag in growth was observed. The lag periods of both species described a saturation curve with pulse dose (E.Spijkerman and P.F.M.Coesel, submitted): the cells took up P until either the pulse was exhausted or the internal maximum cell quota (Q'_{max}) was reached. It was found that *C.abbreviatum* and *S.chaetoceras* were significantly different in Q'_{max} (E.Spijkerman and P.F.M.Coesel, submitted). The lag periods after pulsing in the single-species experiments described in the present paper lasted longer than those described for these species originating from continuously P-limited cultures provided with the same pulse dose (E.Spijkerman and P.F.M.Coesel, submitted). It was not possible to relate the decrease in cell density observed in the period directly after the pulse to the time needed to take up P at $V_{i,max}$ or $V_{lt,max}$. From these observations, we conclude that P uptake and the internal P quota are not the only factors that determine the length of the lag period; probably the history of the cells is also involved. When cells from starved conditions are subjected to a pulse, the lag will possibly last longer than in cells originating from continuously P-limited conditions. Starved cells might require more time for changing cell metabolism from uptake to growth as the starvation has been of longer duration. Time lags in our experiment were of the same order as found by Grover (1991) for *Chlorella* and *Scenedesmus* in similar experiments. Like in his experiments, the lag periods can only be roughly estimated and are therefore hard to relate to concrete physiological characteristics. To acquire more detailed knowledge about the outcome of competition of phytoplankton species under pulsed P limitation, it is necessary to study the characteristics of the lag period more precisely in relation to algal physiology.

The observed difference in maximum cellular P quota (Q'_{max}, being three times higher in *C.abbreviatum* than in *S.chaetoceras*; E.Spijkerman and P.F.M.Coesel, submitted) will result in an advantage for *C.abbreviatum* compared to *S.chaetoceras* with increasing pulse size and time interval between the pulses. Although in none of our pulsed P competition experiments was Q'_{max} reached in either species, the above-predicted phenomenon is roughly shown in Figure 5.

The data presented in Figure 5 are in agreement with the intermediate disturbance hypothesis of Connell (1978). This theory was demonstrated in practice by Robinson and Sandgren (1983), Gaedeke and Sommer (1986) and Sommer (1995), who showed that species richness in their experiments was the highest at an intermediate pulse regime of different nutrients. Applying this intermediate disturbance hypothesis to our results and to the growth strategies as distinguished by Crowley (1975), it can be hypothesized that in the range from continuous nutrient limitation to very frequent, very small pulses, there will be a strong selection in a phytoplankton population favouring affinity-adapted species (high V_{max}/K_m). With increasing pulse interval and larger pulse dose, the velocity-adapted species (high V_{max} and high μ_{max}) will benefit and become dominant, but the fluctuations in different nutrient concentrations offer possibilities for many species to co-exist. However, when pulses become still more pronounced and less frequent, according to our results, selection for the ability to store a limiting nutrient after the pulse (high Q'_{max}/Q_0, Q_0 being the minimum cellular P quota, and low μ_{max}) will possibly become more important, imposing a lower species diversity. From our results with the two desmid species under discussion, we have to conclude that *C.abbreviatum* is the better storage and affinity specialist, compared to *S.chaetoceras* which has more of the characteristics of a velocity specialist. Two different combinations of P pulse and interval size can then be suggested under which the two species possibly co-exist. The first combination, i.e. of small, frequent pulses, was discussed theoretically by Stewart and Levin (1973) and demonstrated to be valid for the two desmid species (Spijkerman and Coesel, 1996b). From Figure 5, co-existence under a second combination, i.e. of big, less frequent pulses, can be derived. Indeed, Hsu (1980) showed theoretically that the co-existence of two competitors might also occur at big pulses at low frequency. However, until now no experimental study on the co-existence of two species under such a pulse regime has been performed.

For both desmid species, a significant adaptation in cell size to the P supply regimes examined could be measured with both Coulter counter and microscope. Both *C.abbreviatum* and *S.chaetoceras* increase their cell volume in response to a larger P addition. Possibly the vacuole increases and, with that, storage ability (Stolte and Riegman, 1995). This finding suggests that cellular storage ability increases with increasing pulse dose (indications of enlarged storage ability under pulsed P limitation were found in our experiments, results not shown). It was found by Suttle *et al.* (1987, Figure 6) that not only the average cell volume in a phytoplankton sample, but also the average cell length of *Synedra radians*, increased with increasing pulse dose. Next to an increase in cell volume of *C.abbreviatum*, a bigger mucus layer around the *Cosmarium* cells was detected under pulsed P conditions. With increasing P limitation, the production

of extracellular polysaccharides is enhanced (Strycek *et al.*, 1992; Domozych *et al.*, 1993). With respect to *C.abbreviatum*, the thickness of the mucus layer was found to decrease at low light intensities (Coesel and Wardenaar, 1994). We observed that the mucilage layer was somewhat thicker under stringent P limitation compared to its size under light-limited conditions (15–22 μm), but the dimensions increased still more when exposed to pulsed P-limited conditions disregarding the size of the pulse. It is possible that the enlargement of the extracellular mucus envelope is another way for *C.abbreviatum* to increase its surface area and, with that, its uptake possibilities for a limiting nutrient after a pulsed addition.

Sommer (1984, 1985) showed in competition experiments that species grown under a pulsed nutrient limitation can react by oscillating as well as by stable cell densities. In our experiments, both *S.chaetoceras* and *C.abbreviatum* oscillated in the pulsed monocultures, showing larger fluctuations with larger pulse dose (comparable to Grover, 1991). Fluctuations in *S.chaetoceras* were larger than those in *C.abbreviatum* and this was best visualized in the competition experiments where cell densities in *S.chaetoceras* were found to oscillate more pronouncedly than in *C.abbreviatum*. Sommer (1984) defined a velocity-adapted species as one showing oscillating densities under pulsed conditions, whereas a storage- or affinity-adapted species would show more stable population densities. Applying this characterization to our data concerning the two desmid species, it is concluded that *S.chaetoceras* tends to a velocity specialist and *C.abbreviatum* to an affinity/storage specialist. This conclusion could already be drawn after measurements on continuous P-limited cultures (Spijkerman and Coesel, 1996a,b), but is strongly supported by the kinetic data from pulsed P conditions provided here.

References

Berger,C. and Sweers,H.E. (1988) The IJsselmeer and its phytoplankton—with special attention to the suitability of the lake as a habitat for *Oscillatoria agardhii* Gom. *J. Plankton Res.*, **10**, 579–599.

Coesel,P.F.M. and Wardenaar,K. (1994) Light-limited growth and photosynthetic characteristics of two planktonic desmid species. *Freshwater Biol.*, **31**, 221–226.

Connell,J.H. (1978) Diversity in tropical rain forests and coral reefs. *Science*, **199**, 1302–1310.

Crowley,P.H. (1975) Natural selection and the Michaelis constant. *J. Theor. Biol.*, **50**, 461–475.

Domozych,C.R., Plante,K., Blais,P., Paliulis,L. and Domozych,D.S. (1993) Mucilage processing and secretion in the green alga *Closterium*. I. Cytology and biochemistry. *J. Phycol.*, **29**, 650–659.

Gaedeke,A. and Sommer,U. (1986) The influence of the frequency of periodic disturbances on the maintenance of phytoplankton diversity. *Oecologia (Berlin)*, **71**, 25–28.

Grover,J.P. (1988) Dynamics of competition in a variable environment: experiments with two diatom species. *Ecology*, **69**, 408–417.

Grover,J.P. (1991) Non-steady state dynamics of algal population growth: experiments with two chlorophytes. *J. Phycol.*, **27**, 70–79.

Hsu,S.B. (1980) A competition model for a seasonally fluctuating nutrient. *J. Math. Biol.*, **9**, 115–132.

Lowry,O.H., Rosebrough,N.J., Farr,A.L. and Randall,R.J. (1951) Protein measurement with the folin phenol reagent. *J. Biol. Chem.*, **193**, 265–275.

Murphy,J. and Riley,J.P. (1962) A modified single-solution method for the determination of phosphate in natural waters. *Anal. Chim. Acta*, **27**, 31–36.

Olsen,Y., Vadstein,O., Andersen,T. and Jensen,A. (1989) Competition between *Staurastrum luetkemuellerii* (Chlorophyceae) and *Microcystis aeruginosa* (Cyanophyceae) under varying modes of phosphate supply. *J. Phycol.*, **25**, 499–508.

Quarmby,L.M., Turpin,D.H. and Harrison,P.J. (1982) Physiological responses of two marine diatoms to pulsed additions of ammonium. *J. Exp. Mar. Biol. Ecol.*, **63**, 173–181.
Riegman,R. and Mur,L.R. (1984) Regulation of phosphate uptake kinetics in *Oscillatoria agardhii*. *Arch. Microbiol.*, **139**, 28–32.
Robinson,J.V. and Sandgren,C.D. (1983) The effect of temporal environmental heterogeneity on community structure: a replicated experimental study. *Oecologia (Berlin)*, **57**, 98–102.
Sokal,R.R. and Rohlf,F.J. (1981) *Biometry*, 2nd edn. W.H.Freeman and Co., New York, 859 pp.
Sommer,U. (1984) The paradox of the plankton: Fluctuations of phosphorus availability maintain diversity of phytoplankton in flow-through cultures. *Limnol. Oceanogr.*, **29**, 633–636.
Sommer,U. (1985) Comparison between steady state and non-steady state competition: Experiments with natural phytoplankton. *Limnol. Oceanogr.*, **30**, 335–346.
Sommer,U. (1991a) A comparison of the Droop and the Monod models of nutrient limited growth applied to natural populations of phytoplankton. *Funct. Ecol.*, **5**, 535–544.
Sommer,U. (1991b) The application of the Droop-model of nutrient limitation to natural phytoplankton. *Verh. Int. Ver. Limnol.*, **24**, 791–794.
Sommer,U. (1995) An experimental test of the intermediate disturbance hypothesis using cultures of marine phytoplankton. *Limnol. Oceanogr.*, **40**, 1271–1277.
Spijkerman,E. and Coesel,P.F.M. (1996a) Phosphorus uptake and growth kinetics of two planktonic desmid species. *Eur. J. Phycol.*, **31**, 53–60.
Spijkerman,E. and Coesel,P.F.M. (1996b) Competition for phosphorus among planktonic desmid species in continuous-flow culture. *J. Phycol.*, **32**, 939–948.
Stewart,F.M. and Levin,B.R. (1973) Partitioning of resources and the outcome of interspecific competition: A model and some general considerations. *Am. Nat.*, **107**, 171–198.
Stolte,W. and Riegman,R. (1995) The effect of phytoplankton cell size on transient state nitrate and ammonium uptake kinetics. *Microbiology*, **141**, 1221–1229.
Strycek,T., Acreman,J., Kerry,A., Leppard,G.G., Nermut,M.V. and Kushner,D.J. (1992) Extracellular fibril production by freshwater algae and cyanobacteria. *Microb. Ecol.*, **23**, 53–74.
Suttle,C.A., Stockner,J.G. and Harrison,P.J. (1987) Effects of nutrient pulses on community structure and cell size of a freshwater phytoplankton assemblage in culture. *Can. J. Fish. Aquat. Sci.*, **44**, 1768–1774.
Swain,W.R., Lingeman,R. and Heinis,F. (1987) A characterization and description of the Maarsseveen Lake system. *Hydrobiol. Bull.*, **21**, 5–16.

Received on April 9, 1997; accepted on August 11, 1997

Journal of Plankton Research Vol.19 no.12 pp.1913–1928, 1997

Estimating growth and mortality in stage-structured populations

Brian J.Rothschild, Alexei F.Sharov, Anthony J.Kearsley[1] and Alexander S.Bondarenko[2]

Center for Marine Sciences and Technology (CMAST), University of Massachusetts at Dartmouth, North Dartmouth, MA 02747, [1]Mathematical and Computational Sciences Division, National Institute of Standards and Technology, Gaithersburg, MD 20899-0001 and [2]Department of Mathematics, University of Massachusetts at Dartmouth, North Dartmouth, MA 02747, USA

Abstract. This paper presents a practical numerical method for separating and estimating growth and mortality coefficients in stage- or size-structured populations using only observations of the relative or absolute abundance of each stage. The method involves writing a system of linear ordinary differential equations (ODEs) modelling the rate of change of abundance. The solution of the differential system can be numerically approximated using standard (e.g. sixth-order Runge–Kutta–Felhberg) methods. An optimization problem whose solutions yield 'optimal' coefficients for a given model is formulated. The ODE numerical integration technique can then be employed to furnish required function and gradient information to the optimization algorithm. The data-fitting software package ODRPACK is then successfully employed to estimate optimal coefficients for the ODE population model. Simulation experiments with four- and eight-stage model populations illustrate that the method results in the successful estimation of coefficients of mortality and growth from abundance data.

Introduction

Growth and mortality are the principal processes that determine population dynamics. Estimation of these life-history parameters at different life stages and time intervals is crucial for understanding and interpreting the changes in population abundance and structure.

However, minimal assumption simple methods for estimating growth rates, mortality rates and stage duration in stage-structured populations require development [see the important contributions by Wood (1994) and by Wood and Nisbet (1991)]. Because methods for estimating such rates are not generally available, many depictions of 'ecosystems' that require such rates use contrived estimates. Furthermore, in the literature, estimates of growth are often confounded with mortality and vice versa; it is necessary to understand the statistical interaction of growth and mortality so that the two vital rates can be separated for use in ecosystem models [the importance of this interaction is discussed in detail by Beyer (1989)].

This paper describes a method for estimating the vital rates and stage duration from estimates of the change in abundance or indices of abundance of each stage as a function of time (as might be obtained from acoustic or optical monitoring methodologies). Subsequent sections illustrate how the abundance trajectories are developed as functions of time from a state diagram, discuss an analytical approach to the problem, demonstrate how mortality-rate and growth-rate parameters can be estimated using an optimization formulation of the problem and

© Oxford University Press

modern parameter estimation software ODRPACK, and describe results of the numerical method applied to the simulated data from four- and eight-stage models. The paper concludes with a discussion.

Problem formulation

The stage-structured approach divides the population into recognizable stages, e.g. nauplii, juvenile or adult stages. It is also possible to think of dividing the population into length classes [as might be appropriate for the study of larval fish; see Beyer (1989)]. The problem is: given estimates of abundance at each stage or length class as a function of time, simultaneously estimate stage- or length-specific mortality and growth rates.

The state diagram in Figure 1 shows the configuration of the problem. The number of organisms in each stage at any instant of time is represented by $x_i(t)$ where i represents the ith stage for $i = 1, \ldots, n$ stages. The vector of x_is at any time t represents the state of the population at time t. The constants $k_{i,i-1}$ represent the growth rates from the $(i-1)$th to the ith stage, while the constants k_{0i} represent the mortality rate of the ith stage.

The dynamics of such a system are represented by the system of linear ordinary differential equations (ODEs):

$$\begin{pmatrix} \dot{x}_1 \\ \dot{x}_2 \\ \vdots \\ \dot{x}_n \end{pmatrix} = \begin{pmatrix} a_{11} & a_{12} & \cdots & a_{1n} \\ a_{21} & a_{22} & \cdots & a_{2n} \\ \vdots & \vdots & & \vdots \\ a_{n1} & a_{n2} & \ddots & a_{nn} \end{pmatrix} \begin{pmatrix} x_1 \\ x_2 \\ \vdots \\ x_n \end{pmatrix} \tag{1}$$

which can be written more compactly as:

$$\dot{\mathbf{x}} = A\mathbf{x}(t) \tag{2}$$

The structure of Figure 1 dictates that in the matrix A, the diagonal elements are $a_{ii} = -(k_{0i} + k_{i+1,i})$. The off-diagonal elements are zero, except for the lower subdiagonal, where $a_{i+1,i} = k_{i+1,i}$. Consider as an example equation (3) representing the dynamics of four life history stages ($n = 4$):

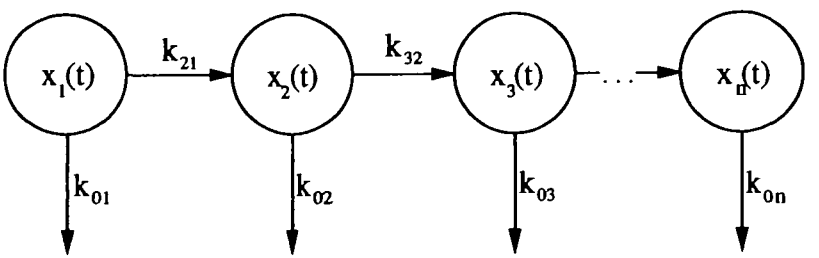


Fig. 1. Stage diagram showing the configuration of the mortality–growth estimate problem.

$$A = \begin{pmatrix} -(k_{01} + k_{21}) & 0 & 0 & 0 \\ k_{21} & -(k_{02} + k_{32}) & 0 & 0 \\ 0 & k_{32} & -(k_{03} + k_{43}) & 0 \\ 0 & 0 & k_{43} & -k_{04} \end{pmatrix} \tag{3}$$

Note that if we can determine a_{11} and a_{21}, for example, then we can determine both the growth and the mortality rates, k_{21} and k_{01}, since $k_{21} = a_{21}$ and $k_{01} = -(a_{11} + a_{21})$, etc.

Note also that $-a_{ii}$ is the total instantaneous loss for the ith stage. The apparent mortality rate is given by $-a_{ii}$. However, if growth is not taken into account, mortality will be overestimated. The magnitude of the overestimates is simply the growth rate $-a_{i,i-1}$ and vice versa.

Matrix stage-based population models were used to solve the 'forward problem'—to forecast population dynamics by multiplying the vector of population abundance by the population projection matrix at each time step (Caswell, 1978, 1980; Crouse *et al.*, 1987; Nakaoka, 1993).

To solve the 'inverse problem', the coefficients of the projection matrix are estimated based on the measurements of the change in abundance or the indices of abundance for each stage.

The problem formulation thus requires a sequence of estimates of abundances for each stage or length class. As a practical model, utilization of this technique may require acoustic or optical estimates. However, because the techniques admit statistical error, problems of misidentification, etc., can be evaluated statistically.

We observe that equation (2) is a linear approximation which seems adequate for relatively short observation intervals and please note that our procedure can be extended to account for non-linear extensions of equation (2).

Analytical solution

The system of linear differential equations (1) can be solved analytically, providing an algebraic expression for abundance $N(t)$ as a function of time t. A straightforward way of solving a system of differential equations (2) is to take its Laplace transform:

$$\mathbf{x}(s) = (sI - A)^{-1}\mathbf{x}(0) \tag{4}$$

where the initial conditions are given by $\mathbf{x}(0) = (K_1, K_2, \ldots, K_n)^t$ and the coefficients in A are unknown parameters. By applying the inverse Laplace transform operator to the solution in algebraic space, we obtain:

$$\mathbf{x}(t) = L^{-1}[(sI - A)^{-1}]\mathbf{x}(0) \tag{5}$$

the time trajectory of the abundance of each life history stage. Standard nonlinear regression can be used to give straightforward estimates of the parameters.

To give the simplest example, consider the two-stage ($n = 2$) population. First, we write the appropriate differential equation:

$$\begin{pmatrix} \dot{x}_1 \\ \dot{x}_2 \end{pmatrix} = \begin{pmatrix} -a & 0 \\ b & -c \end{pmatrix} \begin{pmatrix} x_1 \\ x_2 \end{pmatrix} \tag{6}$$

where a_{11}, a_{21} and a_{22} are represented, respectively, by $-a$, b and $-c$ for notational convenience. We note that $a = k_{01} + k_{21}$, $b = k_{21}$ and $c = k_{02}$. Setting $c = k_{02}$ implies that there is exactly zero growth in the last stage.

Assuming initial conditions $\mathbf{x}(0) = (K_1, K_2)^t$, we solve equation (6) by taking its Laplace transform and then inverting the transform as specified above, which yields:

$$\mathbf{x}(t) = \begin{pmatrix} K_1 e^{-at} \\ \dfrac{K_1 b e^{-at} - K_1 b e^{-ct} + K_2 c e^{-ct} - K_2 a e^{-ct}}{a - c} \end{pmatrix} \tag{7}$$

The first row in the above column vector gives the trajectory or number of individuals as a function of time in the first stage, while the second row in the column vector gives the number of individuals as a function of time in the second stage.

To show the form of equation (7) by an example, let $a = 1.2$, $b = 0.5$, $c = 0.2$, $K_1 = 1000$ and $K_2 = 500$. These trajectories are plotted (see Figure 2). Because $a = 1.2$ and $b = 0.5$, it is clear that $k_{01} = 0.7$ while $k_{21} = 0.5$. This illustrates the

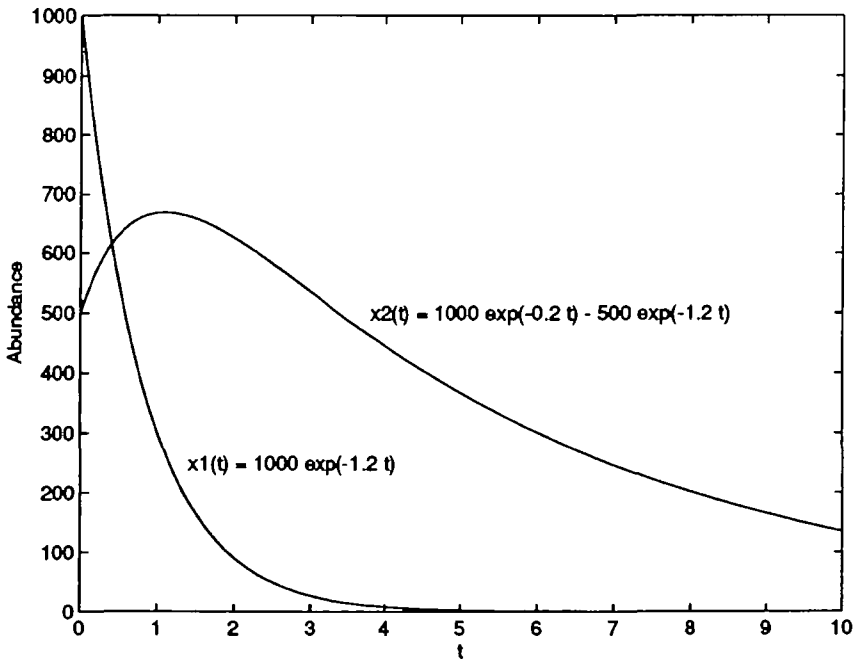


Fig. 2. Abundance of x_1 and x_2 in the two-stage model. They are trajectories according to equations (11) and (12). Note that as x_1 is depleted, x_2 increases. Then x_2 becomes depleted.

separation of growth and mortality constants. Inserting these constants in equation (7) results in:

$$x_1(t) = 1000e^{-1.2t} \tag{8}$$

and

$$x_2(t) = 1000e^{-0.2t} - 500e^{-1.2t} \tag{9}$$

The stage duration can be obtained by simple integration of equations (8) and (9):

$$\bar{T}_i = \int_0^\infty t x_i(t) dt \tag{10}$$

Examination of the stage duration or average time in each stage is interesting because it can be used to calculate the length of the time that the population is exposed to a stage-specific risk. This is particularly important in the theory of larval fish mortality [see the discussion in Rothschild (1986, p. 114)].

To estimate parameters of equation (7), data sets using equations (8) and (9) were simulated and normally distributed noise was added to the data (see Figures 3 and 4).

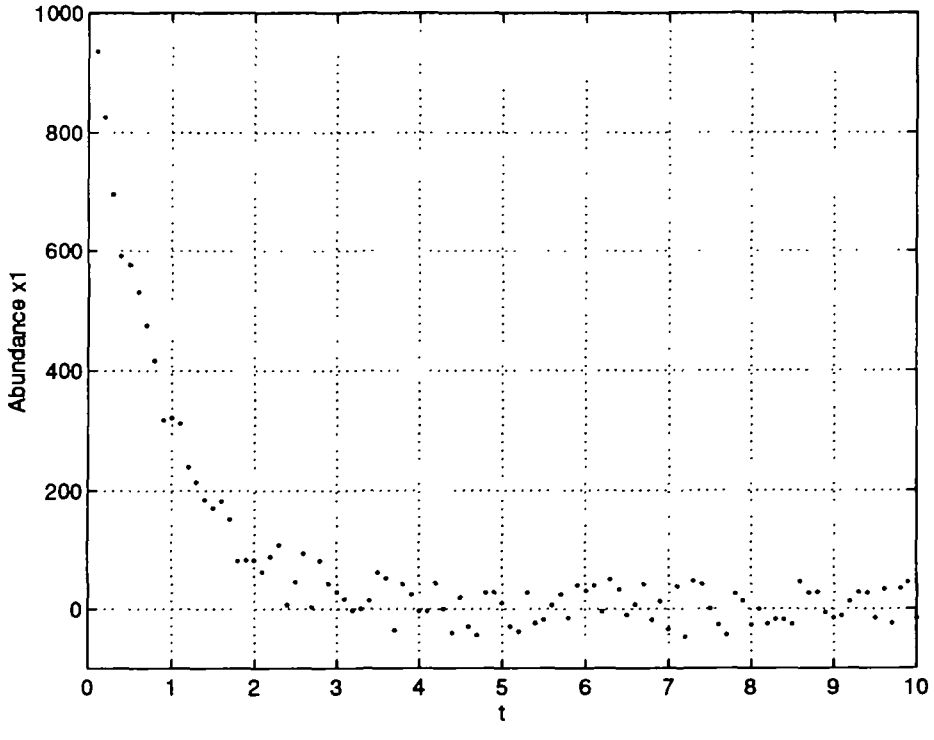


Fig. 3. Simulated abundance dynamics of stage 1 with random noise (two-stage model).

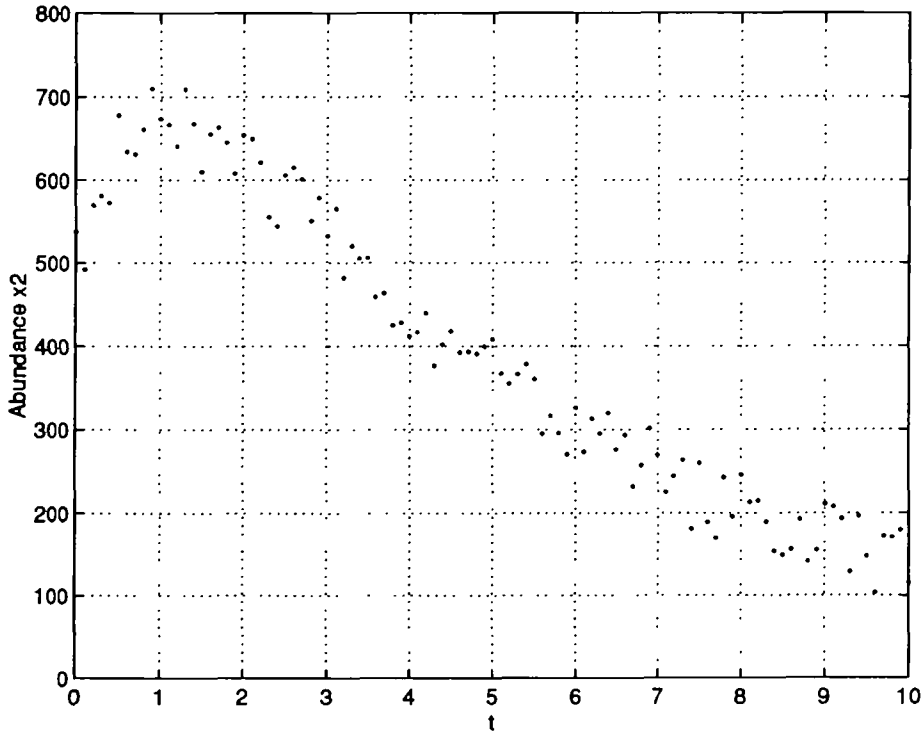


Fig. 4. Simulated abundance dynamics of stage 2 with random noise (two-stage model).

The problem in this 'inverse' approach is now formalized by rewriting equations (8) and (9) in the form:

$$x_1(t) = 1000e^{-\alpha t} \tag{11}$$

and

$$x_2(t) = 1000e^{-\beta t} - 500e^{-\alpha t} \tag{12}$$

Our intent is to estimate the values of α and β. This can be achieved using the standard non-linear regression techniques (Seber and Wild, 1989). Using only the data pictured (in Figures 3 and 4), approximate values of the parameters were recovered with virtually no error.

However, it is interesting to note that with an increase in the number of stages, the equations that need to be solved become more complicated. Perhaps more importantly, with an increase in the number of stages, one runs into the difficulty of generating equations with parameters to be estimated by non-linear regression analysis. Thus, while simple for two-stage population, this approach has significant drawbacks when extended to population models with more than two stages.

Yet, the simple example above highlights the fact that conventional estimates of mortality rate without estimates of growth rate, and estimates of growth rate without estimates of mortality rate, can have substantial systematic biases.

Numerical approach to the problem

Many difficulties with scalability and error estimation in the analytical technique described above for the solution of an ordinary least squares (OLS) problem can be overcome by formulating the problem as an orthogonal distance regression (ODR) problem. The (ODR) problem has been studied [see the papers by Boggs and Rogers (1990) and Boggs *et al.* (1987)] and a robust implementation in public domain software has also been released (Boggs *et al.*, 1989, 1992). The method and implementation have been successfully employed to solve many important application problems. Similarly, below is described the application of ODRPACK to the problem of estimating growth and mortality coefficients in stage-structured populations.

Let $\mathbf{x}_D(t_i)$s denote observed (data) measurements of the numbers of organisms in given stages at times t_i ($i = 1, \ldots, p$). Further, let $\mathbf{x}(t_i)$ approximate the solution to the differential equation (2) comprised of coefficients a_j, $j = 1, \ldots, 2n-1$ (n is the number of stages in the model). In this case, coefficients in the matrix A are enumerated in the following way:

$$A = \begin{pmatrix} a_1 & 0 & 0 & \ldots & 0 \\ a_2 & a_3 & 0 & \ldots & 0 \\ 0 & a_4 & a_5 & \ldots & 0 \\ \vdots & \vdots & \vdots & \ddots & \vdots \\ 0 & 0 & \ldots & a_{2n-2} & a_{2n-1} \end{pmatrix}$$

We wish to minimize the residual sum of the differences between computed and observed data points subject to the computed values satisfying equation (2). The resulting new problem can be formulated:

$$\min_{\mathbf{a}} f(\mathbf{a}) = \sum_{i=1}^{p} \|\mathbf{x}(t_i) - \mathbf{x}_D(t_i)\|_2^2 \tag{13}$$

subject to the constraints

$$A\mathbf{x} = \dot{\mathbf{x}}, \mathbf{x}(0) = (\mathbf{x}_0) \tag{14}$$

$$a_{2i} + a_{2i-1} \leq 0, i = 1, \ldots, n-1 \tag{15}$$

$$a_{2i-1} \leq 0, \; i = 1, \ldots, n \tag{16}$$

The implicit equality constraints (14) require that the coefficients satisfy the appropriate system of differential equations (2), while the inequality constraints

(15) and (16) guarantee that coefficients correspond to the structure of the problem illustrated in equation (3).

Also, since in practice the observation-error variance is proportional to the square of the abundance for mostly process errors and very large samples, we employ the appropriate weighting for the residual sum for the difference between computed and observed data:

$$\min_{\mathbf{a}} f(\mathbf{a}) = \sum_{i=1}^{p} \left\| \frac{\mathbf{x}(t_i) - \mathbf{x}_D(t_i)}{\mathbf{x}_D(t_i)} \right\|_2^2 \tag{17}$$

In short, the problem of approximating the coefficients of our model differential equation has been recast as a constrained optimization problem. The function to be minimized, equation (13), usually called the objective function, is a standard 'output least squares' function. We can write the equality constraints, (14), as one vector function $h(\mathbf{a}) = 0$:

$$h(\mathbf{a}) = (Ax - \dot{x}, x(0) - x_0)^t \tag{18}$$

of our parameters $\mathbf{a}$. Likewise, the inequality constraints can be written as a single vector function, say $g(\mathbf{a}) \leq 0$:

$$g(\mathbf{a}) = (a_{2i} + a_{2i-1}, a_{2i-1})^t \tag{19}$$

Although our constraints are linear, one can easily envision significantly more complicated and certainly highly non-linear ODEs replacing the linear system presently employed. For this reason, we chose to solve this optimization problem numerically (referred to in optimization as a non-linear programming problem) defined by equations (13), (14), (15) and (16) using the standard data-fitting software package ODRPACK (Boggs *et al.*, 1992). Optimization problem (13), (14) can be reformulated without difficulty as an explicit (ODR) problem (see Boggs *et al.*, 1992, p. 4) with implicit constraints (14) rewritten as a model function f:

$$\mathbf{x}(t) = f(t, \mathbf{a}) = A^{-1}\mathbf{x}(t) \tag{20}$$

ODRPACK has been designed for finding the parameters that minimize the sum of the squared weighted orthogonal distances from a set of observations to the curves or surfaces determined by the parameters.

Presently, a drawback of the approach is that one cannot impose constraints. While the problem is not naturally constrained, one can imagine constraints representing maximum or minimum bounds on variations in population in a given cycle or similar constraints. For this reason, the authors are also investigating a constrained optimization approach to the problem employing ideas from sequential quadratic programming (SQP) (see the paper by Boggs *et al.*, 1994). Similar ideas have been successfully employed in other areas of science and engineering (see Kearsley, 1996).

Numerical results

To test the numerical approach, several simulated data sets were generated for both four-stage and eight-stage populations. This was done in the following way:

(i) Coefficients of growth and mortality were randomly picked from the set of reasonable values for growth and mortality rates. We generated 100 coefficient sets for this experiment.
(ii) Numerical solutions of the ODEs with the above coefficients generated a set of observations of abundance of each stage (numerical tests here were performed with $p = 25$ such simulated observations).
(iii) For each coefficient set, 100 levels of normally distributed noise (with standard deviation from 0.16 to 0.24 for four-stage and from 0.09 to 0.12 for eight-stage population models) were added to the simulated data corresponding to random fluctuations within a given percentage of deviation from the 'actual' value (CV of 16–24%), thus generating sets of observations like one would expect to collect in the field. These observations are shown as asterisks, pluses, crosses and circles in Figures 5, 7 and 8.

The resulting data sets were assumed to be the 'observed' data. First we estimated growth and mortality coefficients from the data without the 'noise' using the optimization-based numerical approach described in the previous sections.

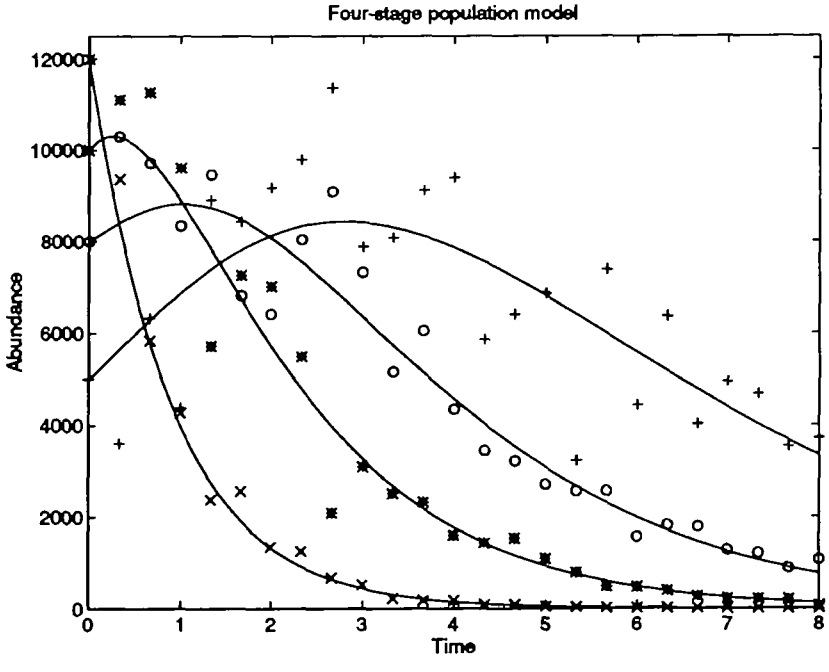


Fig. 5. Simulated abundance dynamics of the four-stage population model. Asterisks, pluses, crosses and circles represent the 'observed' data, and solid lines represent the solution.

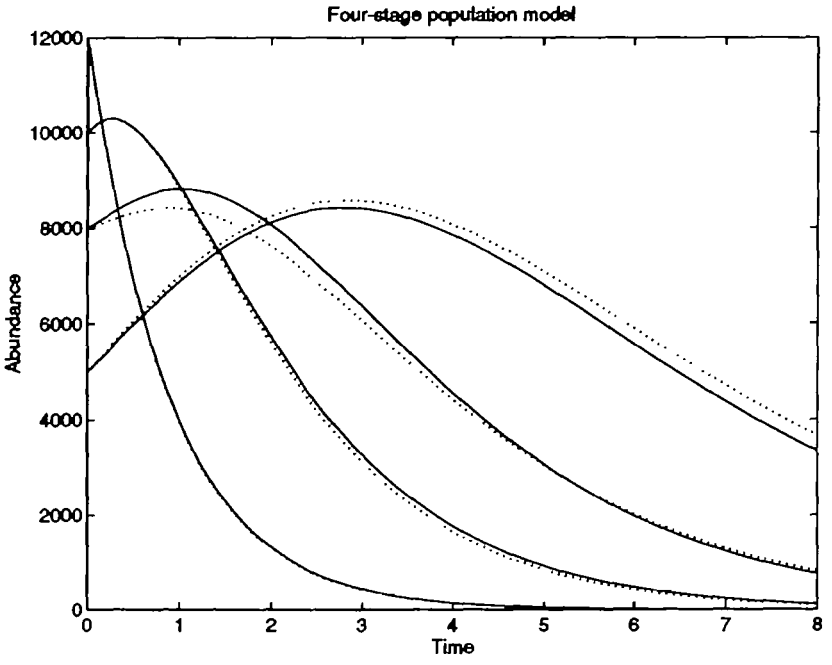


Fig. 6. Typical estimated abundance trajectories (dotted lines) as compared to the original trajectories (solid lines) of the four-stage population model.

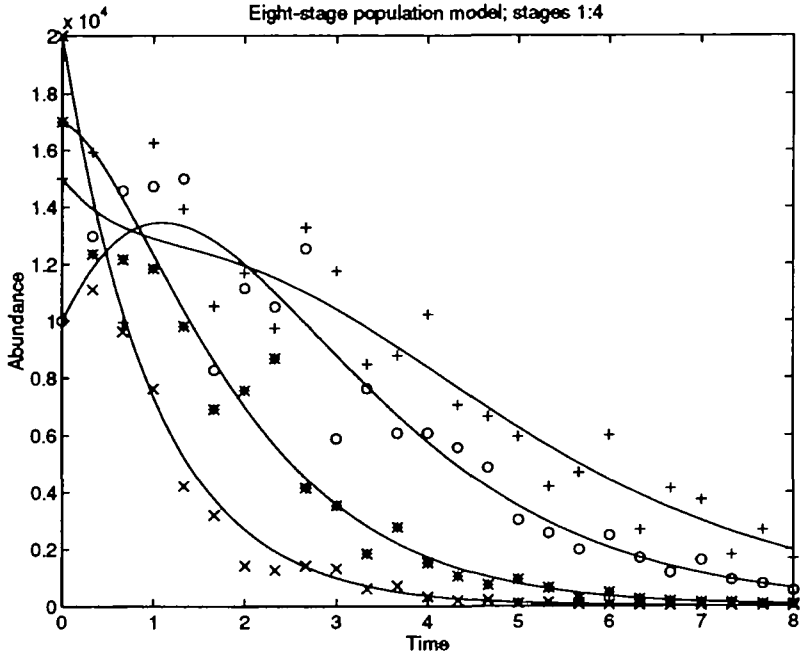
These coefficients were then estimated from the 'observed' data sets using the same numerical approach.

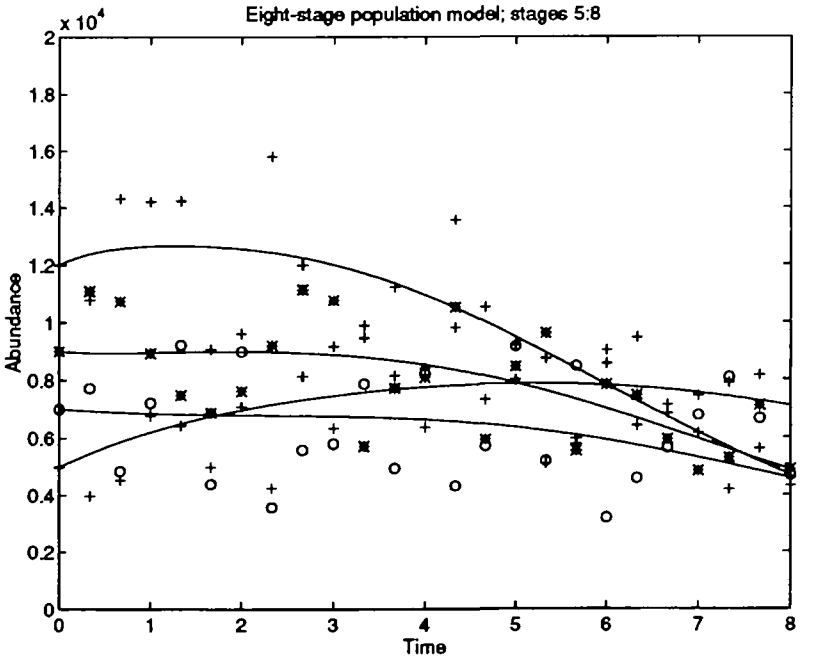
Figures 6, 9 and 10 show the results of the typical estimations from the 'observed' data sets for four- and eight-stage populations. The original trajectories are shown as solid lines and the trajectories produced from the estimated coefficients are shown as dotted lines. Also, Tables I and II show the original and estimated coefficients (with 95% confidence intervals) for these estimations.

As seen from Figures 11 and 12, the accuracy of the estimated coefficients does not appear overly dependent on the level of noise. On the contrary, the CV of coefficients does not appear overly dependent on the level of noise the CV of coefficients remains close to constant as a function of the CV of noise. However, after using our technique to solve identification problems consisting of >100 different coefficient sets, we observed that the selection of a coefficient set greatly influenced the solution and the procedure for finding the solution. In other words, slight perturbations of the coefficient set for which the problem is well conditioned could cause the problem to become ill conditioned.

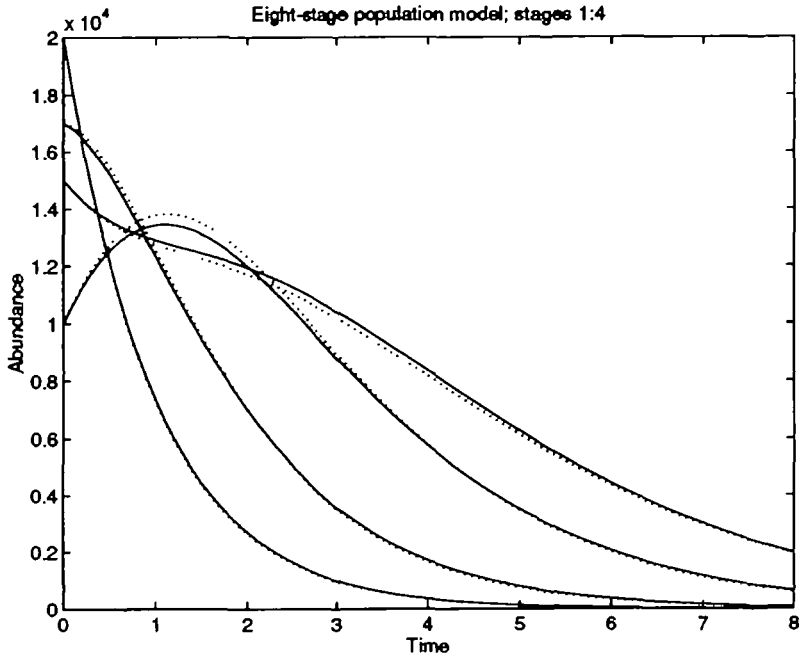
Discussion

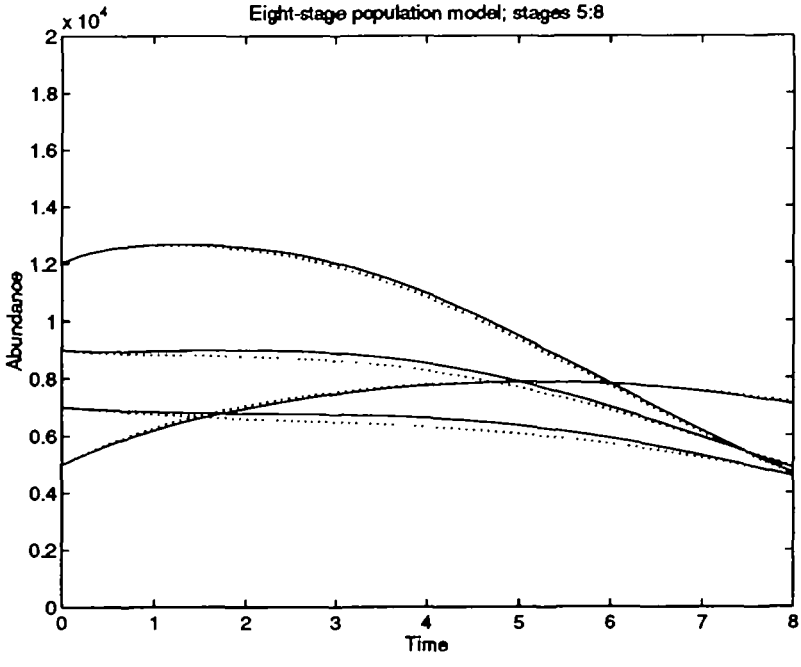
It was shown in numerical experiments that the proposed method allows estimation of rates of mortality and transition to the next stage (growth, maturation, etc.) with sufficient precision. In particular, the scheme appears to work





Figs 7 and 8. Simulated abundance dynamics of the eight-stage population model. Asterisks, pluses, crosses and circles represent the 'observed' data, and solid lines represent the solution.





Figs 9 and 10. Typical estimated abundance trajectories (dotted lines) as compared to the original trajectories (solid lines) of the eight-stage population model.

Table I. Actual and computed coefficients with 95% confidence intervals for the four-stage population model

Actual coefficients	Estimated coefficients	95% confidence intervals
–1.1	–1.10884936	–1.33069617 to –0.88700255
0.8	0.83513807	0.12226160 to 1.54801451
–0.7	–0.72974590	–0.98901686 to –0.47047494
0.6	0.48441035	0.09880331 to 0.87001738
–0.6	–0.52764224	–0.77575753 to –0.27952695
0.5	0.51978080	0.20587469 to 0.83368691
–0.4	–0.38332264	–0.60042499 to –0.16622030

Table II. Actual and computed coefficients with 95% confidence intervals for the eight-stage population model

Actual coefficients	Estimated coefficients	95% confidence intervals
–1.0	–1.01948904	–1.19968538 to –0.83929269
0.7	0.65711214	–0.12456032 to 1.43878460
–0.9	–0.88231027	–1.29305566 to –0.47156484
0.8	0.80611938	0.33502469 to 1.27721408
–0.7	–0.68607393	–0.95137870 to –0.42076916
0.5	0.52101167	–0.09053107 to 1.13255442
–0.6	–0.62544568	–1.12095822 to –0.12993314
0.5	0.50472084	–0.02825008 to 1.03769176
–0.5	–0.51035757	–0.95532174 to –0.06539341
0.5	0.64875412	–0.85221896 to 2.14972721
–0.7	–0.88235942	–2.77042540 to 1.00570655
0.6	0.31064101	–0.85460328 to 1.47588530
–0.8	–0.42090184	–1.87956801 to 1.03776433
0.5	0.67517411	–0.46673167 to 1.81707989
–0.4	–0.56101227	–1.58690365 to 0.46487911

successfully when data are provided in a large number of stages. It appears that casting the model coefficients as solutions to a 'constrained optimization problem' is a viable strategy for finding their approximate values based on observations.

The assumption of constant rates of mortality and growth within each stage is a non-trivial but 'standard' assumption. If the actual process rates are not constant within the stages under consideration, the resulting coefficients would be incorrectly estimated. There are two solutions to this difficulty. The processes could be analysed at shorter time intervals (which means more frequent sampling), such that the rates of mortality and growth could be considered to be constant. Another way to overcome this difficulty is to replace our elementary linear model $\dot{\mathbf{x}} = A\mathbf{x}$ with a more complicated non-linear model $\dot{\mathbf{x}} = \phi(\mathbf{x})$. This is one of the very strong advantages of the numerical approach presented here—in no way does it depend specifically on the particular model employed. Therefore, if we have notions regarding how the process changes in time, we can incorporate these in the selection of appropriate objective and/or constraint functions to be handled by the minimization algorithm.

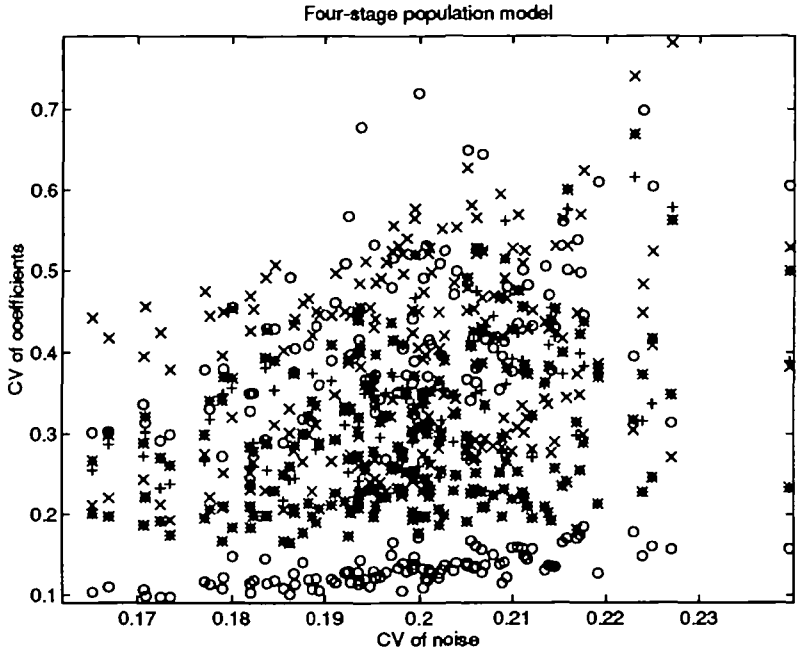


Fig. 11. Uncertainty in estimated coefficients as a function of uncertainty in the population data for the four-stage population model.

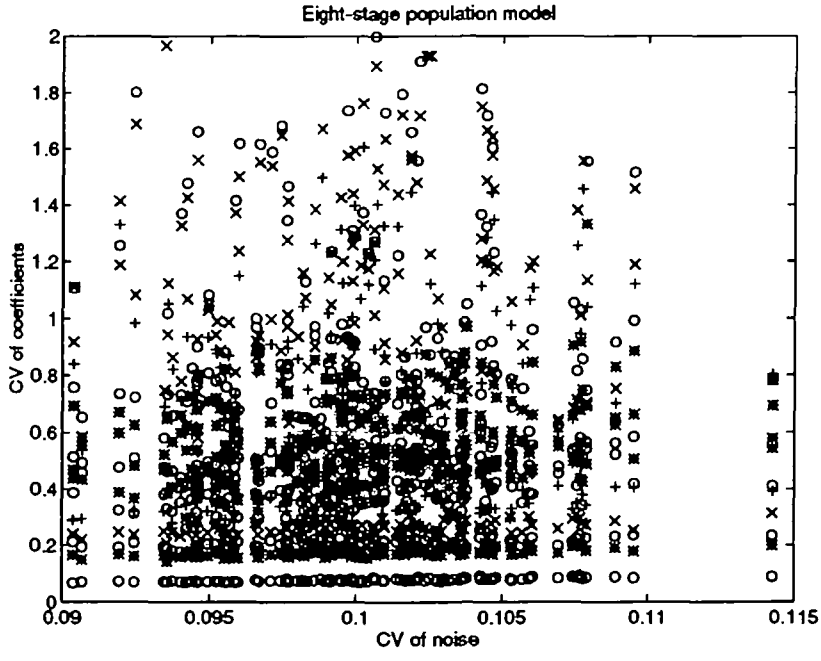


Fig. 12. Uncertainty in estimated coefficients as a function of uncertainty in the population data for the eight-stage population model.

An analysis of larger collections of real field data in terms of the method applicability, development and testing of non-linear models must be conducted. Alternative formulations of our development and testing of non-linear models are the potential perspectives for the future method development. In addition to employing more sophisticated biological models, an examination of potential statistical models that more delicately describe how noise and inaccuracies affect observational data would be of interest.

Finally, we mention that the formulation and numerical solution of parameter identification problems arising in marine sciences is becoming a very active field (for example, see DeAngelis and Coutant, 1979; DeAngelis and Mattice, 1979; Banks *et al.*, 1991; Somerton, 1992). We intend to continue our contribution by studying alternative optimization formulations in search of those that allow more complicated models and demonstrate superior numerical results. The theoretical and numerical characteristics of some alternative formulations are presently being investigated.

Acknowledgements

The authors are extremely grateful to Simon Wood and Mark Bravington for reading this manuscript very thoroughly and making extremely helpful suggestions and corrections. This is a contribution of the National Institute of Standards and Technology (NIST) and is not subject to copyright in the USA. This research was particularly supported by the NOAA, NEFC, CMER programs. The paper is CMAST contribution 97-1001.

References

Banks,H.T., Botsford,L.W., Kappel,F. and Wang,C. (1991) Estimation of growth and survival in size-structured cohort data: an application to larval striped bass (*Morone saxatilis*). *J. Math. Biol.*, **30**, 125–150.

Beyer,J.E. (1989) Recruitment stability and survival—simple size-specific theory with examples from the early life dynamics of marine fish. *Dana*, **7**, 45–147.

Boggs,P.T. and Rogers,J. (1990) Orthogonal distance regression. *Contemp. Math.*, **112**, 183–194.

Boggs,P.T., Byrd,R.H. and Schnabel,R.B. (1987) A stable and efficient algorithm for nonlinear orthogonal distance regression. *SIAM J. Sci. Statist. Comput.*, **8**, 1052–1078.

Boggs,P.T., Byrd,R.H., Donaldson,J.R. and Schnabel,R.B. (1989) Odrpack—software for weighted orthogonal distance regression. *ACM Trans. Math. Software*, 348–364.

Boggs,P.T., Byrd,R.H., Rogers,J.E. and Schnabel,R.B. (1992) User's reference guide for odrpack version 2.01: Software for weighted orthogonal distance regression. Internal report, National Institute of Standards and Technology, Washington DC.

Boggs,P.T., Kearsley,A.J. and Tolle,J.W. (1994) A practical algorithm for general large scale nonlinear optimization problems. Internal report, National Institute of Standards and Technology (to appear in *SIAM Journal on Optimization*, in press).

Caswell,H. (1978) A general formula for the sensitivity of population growth rate to changes in the life history parameters. *Theor. Popul. Biol.*, **14**, 215–230.

Caswell,H. (1980) On the equivalence of maximizing reproductive value and maximizing fitness. *Ecology*, **61**, 19–24.

Crouse,D.T., Crowder,L.B. and Caswell,H. (1987) A stage-based population model for loggerhead sea turtles and implications for conservation. *Ecology*, **65**, 1412–1423.

DeAngelis,D.L. and Coutant,C.C. (1979) Growth rates and size distributions of first year smallmouth bass populations: some conclusions from experiments and a model. *Trans. Am. Fish. Soc.*, **108**, 137–141.

DeAngelis,D.L. and Mattice,J.S. (1979) Implications of a partial differential equation cohort model. *Math. Biosci.*, **47**, 271–285.

Kearsley,A.J. (1996) The use of optimization techniques in the solution of partial differential equations from science and engineering. PhD Thesis, Computational and Applied Mathematics Department, Rice University.

Nakaoka,M. (1993) Yearly variation in recruitment and its effect on population dynamics in *Yoldia notabilis* (Mollusca: Bivalvia), analyzed using projection matrix model. *Res. Popul. Ecol.*, **35**, 199–213.

Rothschild,B.J. (1986) *Dynamics of Marine Fish Populations*. Harvard University Press, Cambridge MA.

Seber,G.A.F. and Wild,C.A. (1989) *Nonlinear Regression*. Wiley and Sons, New York.

Somerton,D.A. (1992) Inverse method for mortality and growth estimation: a new method for larval fishes. *Fish. Bull.*, **90**, 368–375.

Wood,S.N. (1994) Obtaining birth and mortality patterns from structured population trajectories. *Ecol. Monogr.*, **64**, 23–44.

Wood,S.N. and Nisbet,R.M. (1991) Estimation of mortality rates in size structured populations. *Lecture Notes Biomath.*, **90**, 1–101.

Received on September 30, 1996; accepted on August 12, 1997